

Shaping wave patterns in reaction-diffusion systems

Jakob Löber,^{*} Steffen Martens, and Harald Engel
*Institut für Theoretische Physik, Hardenbergstraße 36, EW 7-1,
Technische Universität Berlin, 10623 Berlin, Germany*

We present a method to control the two-dimensional shape of traveling wave solutions to reaction-diffusion systems, as e.g. interfaces and excitation pulses. Control signals that realize a pre-given wave shape are determined analytically from nonlinear evolution equation for isoconcentration lines as the perturbed nonlinear phase diffusion equation or the perturbed linear eikonal equation.

While the control enforces a desired wave shape perpendicular to the local propagation direction, the wave profile along the propagation direction itself remains almost unaffected. Provided that the one-dimensional wave profile of all state variables and its propagation velocity can be measured experimentally, and the diffusion coefficients of the reacting species are given, the new approach can be applied even if the underlying nonlinear reaction kinetics are unknown.

PACS numbers: 82.40.Ck, 02.30.Yy, 82.40.Bj

I. INTRODUCTION

Complex wave patterns in reaction-diffusion systems can often be understood as being assembled of simple “building blocks” as traveling fronts and pulses. A one-dimensional solitary pulse in the FitzHugh-Nagumo model can be considered as being built of two propagating interfaces separating the excited from the refractory state [1]. These interfaces are front solutions to a simpler reaction-diffusion system. Similarly, many two-dimensional shapes can be approximated as consisting of appropriately shifted one-dimensional pulse profiles. A reduced description entirely neglects the explicit form and dynamics of the pulse profile and rather describes the shape of the pattern in terms of a curve outlining it. Several evolution equations for this time-dependent curve, called equations of motion (EOM) throughout this article, can be derived directly from the reaction-diffusion system [2–5].

The control of patterns in reaction-diffusion system has received the attention of many researchers in the past [6, 7]. For example, different feedback control loops have been realized in experiments with the photosensitive Belousov-Zhabotinsky (BZ) reaction [8] using feedback signals obtained from wave activity measured at one or several detector points, along detector lines, or in a spatially extended control domain including global feedback control [9–11]. Furthermore, feedback-mediated control loops can be employed in order to stabilize unstable patterns, such as unstable traveling wave segments and spots. Two feedback loops were used to guide unstable wave segments in the BZ reaction along pre-given trajectories [12, 13]. An open loop control was successfully deployed in dragging traveling chemical pulses of adsorbed CO during heterogeneous catalysis on platinum single crystal surfaces [14]. In these experiments, the pulse velocity was controlled by a laser beam creating a

movable localized temperature heterogeneity on an addressable catalyst surface, resulting in a V-shaped pattern [15, 16]. Dragging a one-dimensional chemical front or phase interface to a new position by anchoring it to a movable parameter heterogeneity, was studied theoretically in [17–19].

Recently we developed a method to control the position over time of one-dimensional traveling waves in reaction-diffusion systems by spatio-temporal forcing [20]. We utilized an ordinary differential equation for the wave’s position over time in response to an external perturbation. Using this equation, we formulated an inverse problem for the control signal enforcing the traveling wave to follow a desired protocol of motion. We demonstrated by example that the analytically obtained control function is close to the numerical solution of an appropriately formulated optimal control algorithm [21–23]. Furthermore, we identified the mechanism leading to a successful position control and thereby proved stability of position control with respect to perturbations of the initial position on the reduced level of the one-dimensional EOM [24].

In this article we extend position control to shape control of two-dimensional wave patterns. In Sec. II, EOMs for two-dimensional traveling waves under perturbations are motivated. We demonstrate how these equations can be utilized to control the shape of a nearly planar traveling wave in Sec. III, and of more complex wave patterns in Sec. IV. In Sec. V we discuss which additional control terms have to act on the boundary of a finite domain to guide traveling waves from the outside to the inside of a domain or vice versa. We end with conclusions in Sec. VI.

II. EQUATION OF MOTION FOR TWO-DIMENSIONAL TRAVELING WAVES

We consider a perturbed reaction-diffusion (RD) system for the vector of n species $\mathbf{u} = \mathbf{u}(\mathbf{r}, t) = (u_1(\mathbf{r}, t), \dots, u_n(\mathbf{r}, t))^T$ in a two-

^{*} jakob@physik.tu-berlin.de

dimensional medium with position vector $\mathbf{r} = (x, y)^T$,

$$\partial_t \mathbf{u} = \mathcal{D} \Delta \mathbf{u} + \mathbf{R}(\mathbf{u}) + \epsilon \mathcal{G}(\mathbf{u}) \mathbf{f}(\mathbf{r}, t). \quad (1)$$

Here, \mathcal{D} is a diagonal matrix of constant diffusion coefficients and Δ denotes the Laplacian operator. The spatiotemporal perturbations \mathbf{f} are coupled by a (possibly \mathbf{u} -dependent) matrix \mathcal{G} into the system, and \mathbf{R} describes a nonlinear reaction kinetics. The small parameter ϵ ensures that the perturbation couples weakly to the system and can be used for a perturbation expansion [20]. The medium is assumed to be isotropic, infinitely extended in the x -direction, and finite with domain size L_y in the y -direction. Homogeneous Neumann boundary conditions are applied in the y -direction,

$$\partial_y \mathbf{u}(x, 0, t) = \partial_y \mathbf{u}(x, L_y, t) = 0. \quad (2)$$

Solutions of interest of the unperturbed ($\epsilon = 0$) RD system Eq. (1) are planar traveling waves \mathbf{U}_c . We fix the propagation direction of the unperturbed wave to be the x -direction such that $\mathbf{U}_c(\xi)$ is a stationary solution in a frame of reference $\xi = x - ct$ comoving with velocity c ,

$$0 = \mathcal{D} \partial_\xi^2 \mathbf{U}_c(\xi) + c \partial_\xi \mathbf{U}_c(\xi) + \mathbf{R}(\mathbf{U}_c(\xi)). \quad (3)$$

Upon a perturbation expansion of Eq. (1) around the traveling wave solution \mathbf{U}_c , the linear operator

$$\mathcal{L} = \mathcal{D} \partial_\xi^2 + c \partial_\xi + \mathbb{D} \mathbf{R}(\mathbf{U}_c(\xi)), \quad (4)$$

arises [3, 25]. The derivative of the unperturbed wave profile $\mathbf{U}_c(\xi)$ with respect to ξ , $\mathbf{W}(\xi) = \mathbf{U}'_c(\xi)$, is an eigenfunction of the operator \mathcal{L} to eigenvalue zero,

$$\mathcal{L} \mathbf{U}'_c(\xi) = 0, \quad (5)$$

known as the Goldstone mode. The existence of the Goldstone mode corresponds to the invariance of the unperturbed RD system with respect to spatial translations in the x -direction. We assume $\mathbf{U}_c(\xi)$ to be a *stable* traveling wave solution such that the zero eigenvalue of \mathcal{L} , $\lambda_0 = 0$, is the eigenvalue with largest real part. Furthermore, we suppose the existence of a spectral gap, i.e., the eigenvalue λ_1 of \mathcal{L} with next largest real part is separated by a finite distance from the imaginary axis.

For what follows we also need the adjoint Goldstone mode or response function $\mathbf{W}^\dagger(x)$ [26] defined as the eigenfunction to eigenvalue 0 of the adjoint operator \mathcal{L}^\dagger of \mathcal{L} ,

$$\mathcal{L}^\dagger = \mathcal{D} \partial_\xi^2 - c \partial_\xi + \mathbb{D} \mathbf{R}(\mathbf{U}_c(\xi))^T, \quad (6)$$

$$\mathcal{L}^\dagger \mathbf{W}^\dagger = 0. \quad (7)$$

For single component RD systems with scalar diffusion coefficient $\mathcal{D} = D$, a general expression for the response function in terms of the traveling wave profile U_c reads

$$\mathbf{W}^\dagger(\xi) = e^{c\xi/D} U'_c(\xi), \quad (8)$$

while in the multi-component case no general expression is known.

Perturbations can deform both the profile \mathbf{U}_c and the shape of a traveling plane wave solution. We neglect deformations of the wave profile \mathbf{U}_c and describe the deviations from the planar wave shape by a time-dependent curve $\gamma(s, t) = (\gamma_x(s, t), \gamma_y(s, t))^T$ tracing out a chosen isoconcentration line parametrized by s . This curve specifies the position of a traveling wave in two spatial dimensions. For a monotonically decreasing front solution, we define its position as the point of steepest slope, while the position of a pulse solution is given by the point of maximum amplitude of an arbitrary component. For an unperturbed plane wave solution propagating with velocity c in the x -direction, the curve γ is a straight line given by

$$\gamma(y, t) = \begin{pmatrix} ct \\ y \end{pmatrix}, \quad (9)$$

where y denotes the Cartesian coordinate transversal to the propagation direction. A local velocity for each point of the curve can be defined as (throughout the article, the time derivative is indicated by the dot while the prime denotes the derivative with respect to the spatial variable)

$$\mathbf{v}(s, t) = \dot{\gamma}(s, t). \quad (10)$$

For a straight line, this yields a velocity $\mathbf{v}(y, t) = c \mathbf{e}_x$ which is constant along the curve and equals the overall velocity c of the plane wave.

Using multiple scale perturbation theory, an evolution equation for $\gamma(s, t)$ can be derived from the perturbed RD system Eq. (1). We suppose the following parametrization for γ

$$\gamma(y, t) = \begin{pmatrix} \phi(y, t) \\ y \end{pmatrix}, \quad (11)$$

to obtain an equation for the x -component of the position $\phi(y, t)$. The ansatz

$$\phi(y, t) = ct + \Phi(Y, T). \quad (12)$$

assumes a fast dynamics on the time scale t which corresponds to the ordinary one-dimensional propagation of the unperturbed plane wave with velocity c . In a frame comoving with velocity c , all variations, denoted by Φ , are assumed to be slow. Consequently, Φ depends on the slow time scale $T = \epsilon t$. Furthermore, it is assumed that the curve γ varies only weakly along the transversal direction, i.e., Φ depends solely on the stretched spatial coordinate $Y = \epsilon^{1/2} y$ [2]. The small parameter ϵ fixes the time and space scale on which the curve γ changes in the comoving frame as well as the amplitude of the perturbation in Eq. (1). Because of the presumed existence of a spectral gap of \mathcal{L} , deformations of the pulse profile in response to the perturbation decay fast and can be neglected [20]. These assumptions yield a closed EOM for $\phi(y, t)$ [2],

$$\dot{\phi} = c + \frac{c}{2}(\phi')^2 + \alpha\phi'' - \frac{\epsilon}{K_c} \int_{-\infty}^{\infty} dx \mathbf{W}^{\dagger T}(x) \mathcal{G}(\mathbf{U}_c(x)) \mathbf{f}(\mathbf{r} + \phi \mathbf{e}_x, t), \quad (13)$$

with the constants

$$K_c = \langle \mathbf{W}^{\dagger}, \mathbf{U}'_c \rangle = \int_{-\infty}^{\infty} dx \mathbf{W}^{\dagger T}(x) \mathbf{U}'_c(x), \quad (14)$$

$$\alpha = \frac{\langle \mathbf{W}^{\dagger}, \mathcal{D}\mathbf{U}'_c \rangle}{\langle \mathbf{W}^{\dagger}, \mathbf{U}'_c \rangle} = \frac{1}{K_c} \int_{-\infty}^{\infty} dx \mathbf{W}^{\dagger T}(x) \mathcal{D}\mathbf{U}'_c(x). \quad (15)$$

and initial condition

$$\phi(y, t_0) = \phi_0(y). \quad (16)$$

A detailed derivation of Eq. (13) is given in Appendix A. For simplicity, we assume ϕ to be a single valued function of y . This excludes any overhangs and in particular closed curves γ . Therefore an isoconcentration line described by γ has to start and end at the domain boundaries. A Neumann boundary condition, Eq. (2), for the RD system (1) implies a right angle between any isoconcentration line and the domain boundary and translates to a Neumann boundary for ϕ ,

$$\partial_y \phi(0, t) = \partial_y \phi(L_y, t) = 0. \quad (17)$$

The unperturbed ($\epsilon = 0$) version of Eq. (13) is known as the nonlinear phase diffusion equation [2, 4]. This nonlinear PDE can be transformed to the linear diffusion equation via the Cole-Hopf transform. The nonlinear term $\sim (\phi')^2$ in Eq. (13) has a purely geometric origin while the second order derivative $\sim \phi''$ describes relaxation of the curve to a straight line with a surface tension α , Eq. (15). Note that for a single component RD system with scalar diffusion coefficient $\mathcal{D} = D$ follows $\alpha = D > 0$. Negative values of α can occur in unperturbed RD systems of activator-inhibitor type if the inhibitor diffuses much faster than the activator [27, 28]. For $\alpha < 0$ plane wave solutions become unstable, undergoing a transversal wave instability. Introducing a fourth order derivative $\sim \partial_y^4 \phi$ in the unperturbed ($\epsilon = 0$) Eq. (13) leads to the Kuramoto-Sivashinsky equation which can describe patterns arising beyond the onset of transversal instabilities [2, 29]. A variation of Eq. (13) with a spatially distributed Gaussian white noise term instead of the perturbation is known as the Kardar-Parisi-Zhang equation [30].

For plane waves ϕ does not depend on y and the perturbed nonlinear phase diffusion equation (13) reduces to the one-dimensional case

$$\dot{\phi}(t) = c - \frac{\epsilon}{K_c} \int_{-\infty}^{\infty} dx \mathbf{W}^{\dagger T}(x) \mathcal{G}(\mathbf{U}_c(x)) \mathbf{f}(x + \phi(t), t), \quad (18)$$

which has been intensively studied in [31–37].

III. SHAPING A PLANE WAVE

Usually the EOM (13) is seen as a PDE for the wave shape $\phi(y, t)$. However, here we utilize Eq. (13) to formulate the inverse problem. Namely, we are looking for the control signal \mathbf{f} given as a solution to the integral equation (13) for a prescribed function $\phi(y, t)$ outlining the shape of the pattern to be enforced [20].

Many inverse problems are mathematically ill posed as they do not yield a unique solution. This holds in our case, too. Therefore, we have to rely on some physical insight to pick a meaningful solution. We start from a fairly general solution involving some arbitrary functions which are then fixed in a second step. Below, we set $\epsilon = 1$, assuming the control signal \mathbf{f} is sufficiently small in amplitude. Furthermore, we suppose that the wave moves unperturbed until the initial time $t = t_0$ upon which the control is switched on. The initial shape of the wave is not necessarily a plane wave $\phi(y, t_0) = \phi_0(y)$.

We rearrange Eq. (13) in the form

$$K_c \left(c - \dot{\phi} + \frac{c}{2}(\phi')^2 + \alpha\phi'' \right) = \int_{-\infty}^{\infty} dx \mathbf{W}^{\dagger T}(x) \mathcal{G}(\mathbf{U}_c(x)) \mathbf{f}(\mathbf{r} + \phi \mathbf{e}_x, t). \quad (19)$$

The left hand side is a sum over four terms, thus, to be as general as possible, we assume a superposition of four independent contributions to the control term \mathbf{f} according to

$$\mathbf{f}(\mathbf{r}, t) = \mathcal{G}^{-1}(\mathbf{U}_c(x - \phi)) \sum_{i=1}^4 \mathcal{A}_i(y, t) \mathbf{h}_i(x - \phi). \quad (20)$$

To eliminate the coupling matrix \mathcal{G} , all terms are multiplied by the inverse \mathcal{G}^{-1} . Because all terms depending on the x -coordinate are evaluated at $x - \phi$, ϕ can be eliminated by a simple substitution in the integral on the right hand side of Eq. (19). The terms $\mathcal{G}^{-1}(\mathbf{U}_c(x - \phi)) \mathbf{h}_i(x - \phi)$ are constant in the comoving frame of reference of the controlled traveling wave while the control amplitude is determined by the terms $\mathcal{A}_i(y, t)$. We are left with

$$K_c \left(c - \dot{\phi} + \frac{c}{2}(\phi')^2 + \alpha\phi'' \right) = \sum_{i=1}^4 \mathcal{A}_i(y, t) \langle \mathbf{W}^{\dagger}(x), \mathbf{h}_i(x) \rangle. \quad (21)$$

Every term on the right hand side cancels exactly one term on the left hand side if we set

$$\begin{aligned} \mathcal{A}_1(y, t) &= c \frac{K_c}{G_1}, & \mathcal{A}_2(y, t) &= -\dot{\phi} \frac{K_c}{G_2}, \\ \mathcal{A}_3(y, t) &= \frac{c}{2}(\phi')^2 \frac{K_c}{G_3}, & \mathcal{A}_4(y, t) &= \alpha\phi'' \frac{K_c}{G_3}, \end{aligned} \quad (22)$$

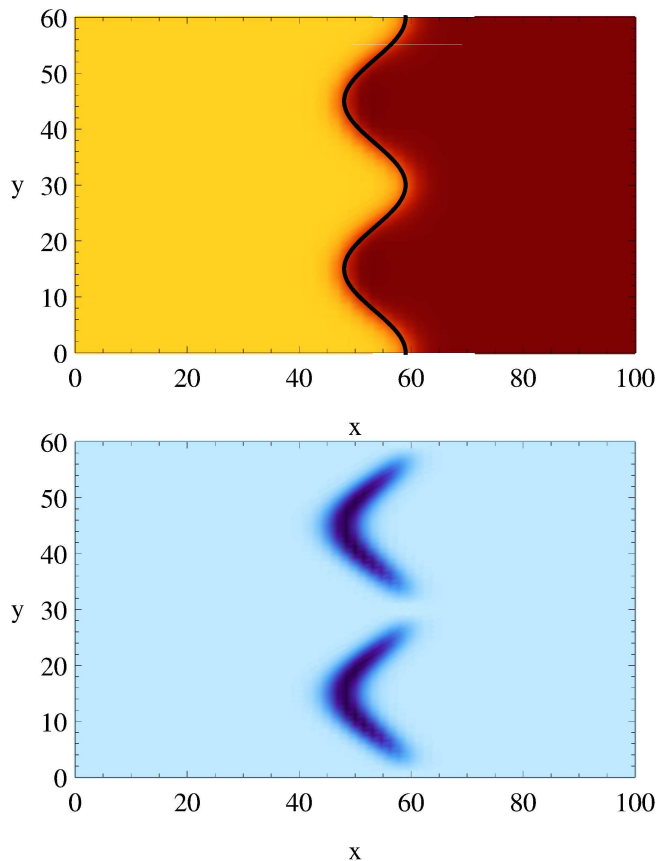


Figure 1. (Color online) Top: Shaping a Schlögl front according to a protocol $\phi(y, t)$ (black line). Yellow (red) corresponds to a high (low) value of u . Bottom: Corresponding control function $f(\mathbf{r}, t)$. Blue (black) corresponds to a high (low) value of f . See movie in the Supplemental Material [38].

with

$$G_i = \langle \mathbf{W}^\dagger(x), \mathbf{h}_i(x) \rangle = \int_{-\infty}^{\infty} dx \mathbf{W}^{\dagger T}(x) \mathbf{h}_i(x). \quad (23)$$

Equation (20) together with Eq. (22) and Eq. (23) constitutes the most general solution for the control function \mathbf{f} . This solution contains four arbitrary vector-valued functions $\mathbf{h}_i(x)$. Because a perturbation proportional to the Goldstone mode, $\mathbf{f} \sim \mathbf{U}'_c$, shifts the traveling wave as a whole [20], we choose

$$\mathbf{h}_i(x) = \mathbf{U}'_c(x), \quad i \in \{1, \dots, 4\} \quad (24)$$

and get

$$\mathbf{f} = \left(c - \dot{\phi} + \frac{c}{2}\phi'^2 + \alpha\phi'' \right) \mathcal{G}^{-1}(\mathbf{U}_c(x - \phi)) \mathbf{U}'_c(x - \phi). \quad (25)$$

Note that the constants G_i involving the response function $\mathbf{W}^\dagger(x)$ cancel out because $G_c = K_c$ for this choice.

This is of great advantage because, in general, the response function can only be determined numerically from the one-dimensional RD equations, or by repeated measurements of traveling waves in a well defined experimental setup. However, the coefficient α , Eq. (15), still depends on the response function. To get rid of α , we choose a slightly different solution with

$$\mathbf{h}_i(x) = \mathbf{U}'_c(x), \quad i \in \{1, \dots, 3\}, \quad (26)$$

$$\mathbf{h}_4(x) = \mathcal{D}\mathbf{U}'_c(x), \quad (27)$$

and find the following solution for the control

$$\mathbf{f} = \mathcal{G}^{-1}(\mathbf{U}_c(x - \phi)) \left(\left(c - \dot{\phi} + \frac{c}{2}\phi'^2 \right) \mathbf{U}'_c(x - \phi) + \phi'' \mathcal{D}\mathbf{U}'_c(x) \right). \quad (28)$$

Instead of the (unknown) coefficient α , Eq. (28) contains the matrix of diffusion coefficients \mathcal{D} . Note that for the single component case with scalar diffusion coefficient $\mathcal{D} = D$ we obtain $\alpha = D$ and Eq. (28) is equivalent to Eq. (25).

In the following, we apply the shape control Eq. (25) to the front solution of the Schlögl model [39],

$$\partial_t u = \Delta u - u(u - a)(u - 1). \quad (29)$$

The Schlögl model is a simple example of a single component RD system exhibiting bistability. Initially, Eq. (29) has been discussed in 1938 by Zeldovich and Frank-Kamenetsky in connection with flame propagation [40]. The one-dimensional front solution connects the homogeneous steady state $u = 1$ for $x \rightarrow -\infty$ and $u = 0$ for $x \rightarrow \infty$. The front profile is known analytically [41]

$$U_c(\xi) = 1 / (1 + \exp(\xi/\sqrt{2})) \quad (30)$$

and the associated propagation velocity is given by

$$c = \frac{1}{\sqrt{2}}(1 - 2a). \quad (31)$$

As an example, we choose an additive control, i.e., a constant coupling function $\mathcal{G}(u) = 1$, in the control signal Eq. (25).

Starting from a plane front traveling in the x -direction at $t = t_0$, we want the control to enforce a transition to a sinusoidally shaped stationary front at time $t = t_1$. The corresponding protocol for $t_0 \leq t \leq t_1$ is

$$\phi(y, t) = \phi_0 + A \cos\left(4\pi \frac{y}{L_y}\right) \sin\left(\frac{\pi}{2} \frac{t - t_0}{t_1 - t_0}\right). \quad (32)$$

In numerical simulations, we set $L_y = 60$ for the domain size in the y -direction, $t_1 - t_0 = 300/4$ for the time span and $A = 50/(2\pi)$ for the amplitude. Starting at time t_1 , the protocol is frozen as $\phi(y, t_1)$ to maintain a sinusoidally modulated stationary front; cf. the movie in [38]. Fig. 1 displays a snapshot showing the time evolution of a Schlögl front under the control. The shape of the front, given by the points of steepest slope of the front profile, closely follows the protocol (black solid line), see Fig. 1 top. The corresponding control function attains its largest amplitude at the points where the modulated shape deviates most from a plane wave, see Fig. 1 bottom.

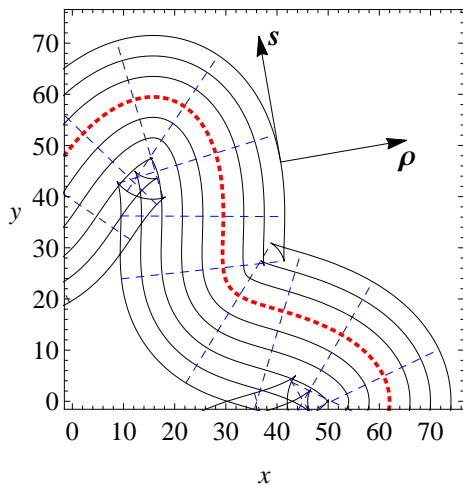


Figure 2. (Color online) Time-dependent local coordinate system (ρ, s) used for the derivation of the linear eikonal equation. Dashed blue lines are contours with $s = \text{const.}$, black solid lines are contours with $\rho = \text{const.}$ The red dotted line denotes the curve $\gamma(s, t)$ which corresponds to the contour with $\rho = 0$. $\gamma(s, t)$ defines the position of the traveling wave in two spatial dimensions and outlines the desired shape of the controlled wave pattern.

IV. SHAPING ARBITRARY WAVE PATTERNS

The nonlinear phase diffusion equation (13) arises through a perturbation expansion around a one-dimensional traveling wave propagating in the x -direction. Naturally, we expect Eq. (13) to fail if the local propagation direction of the perturbed wave is very different from the x -direction. For example, a plane wave traveling in the y -direction cannot be a solution to Eq. (13). Furthermore, we also want to describe and control wave patterns outlined by a closed curve $\gamma(s, t)$. A generalized EOM, known as the linear eikonal equation, accounts for such cases. To derive the latter, a local coordinate system in terms of the coordinates s and ρ is constructed,

$$\mathbf{r} = \begin{pmatrix} x(\rho, s, t) \\ y(\rho, s, t) \end{pmatrix} = \boldsymbol{\chi}(\rho, s, t) = \boldsymbol{\gamma}(s, t) + \rho \mathbf{n}(s, t). \quad (33)$$

Here $\mathbf{n}(s, t)$ is the normal vector of $\boldsymbol{\gamma}$,

$$\mathbf{n}(s, t) = \frac{\boldsymbol{\gamma}''(s, t)}{\sqrt{\boldsymbol{\gamma}''(s, t) \cdot \boldsymbol{\gamma}''(s, t)}}. \quad (34)$$

In contrast to the nonlinear phase diffusion equation, which assumes a fixed propagation direction of the unperturbed traveling wave, here propagation is along the normal direction which is allowed to vary in time and space. The leading order solution to the RD system expressed in the new coordinates is the one-dimensional traveling wave solution $\mathbf{U}_c(\rho)$. See Fig. 2 for a visualization of the coordinate system Eq. (33).

The normal velocity c_n along the curve $\boldsymbol{\gamma}$ is defined as

$$c_n(s, t) = \mathbf{n}(s, t) \cdot \dot{\boldsymbol{\gamma}}(s, t), \quad (35)$$

while its curvature $\kappa(s, t)$ is given by

$$\kappa = \frac{\gamma'_x \gamma''_y - \gamma'_y \gamma''_x}{\left((\gamma'_x)^2 + (\gamma'_y)^2 \right)^{3/2}}. \quad (36)$$

The linear eikonal equation relates the normal velocity c_n along the curve $\boldsymbol{\gamma}$ to its local curvature κ ,

$$c_n(s, t) = c - \alpha \kappa(s, t). \quad (37)$$

Recently, Dierckx et al. [5] derived higher order corrections to Eq. (37) and generalized it to anisotropic media. In particular, they showed that for isotropic media the coefficient α is indeed given by expression (15).

Equation (37) is a coordinate-free expression for the evolution law of $\boldsymbol{\gamma}(s, t)$. To account for the effect of a spatio-temporal perturbation $\mathbf{f}(\mathbf{r}, t)$, we suggest the following generalization of Eq. (37),

$$c_n(s, t) = c - \alpha \kappa(s, t) - \frac{\epsilon}{K_c} \int_{-\infty}^{\infty} d\rho \mathbf{W}^{\dagger T}(\rho) \mathcal{G}(\mathbf{U}_c(\rho)) \mathbf{f}(\boldsymbol{\chi}(\rho, s, t), t). \quad (38)$$

The integration is performed over the coordinate ρ longitudinal to the local propagation direction. The perturbative term is a direct generalization of the corresponding term in the perturbed nonlinear phase diffusion equation Eq. (13). Supposing the same time and space scale separation as in Sec. II and Appendix A, one obtains the perturbed phase diffusion equation (13) from the perturbed linear eikonal equation (38) (see Appendix B for a detailed derivation). Furthermore, the derivation reveals that the curvature coefficient α in Eq. (38) indeed equals the coefficient in front of the 2nd order derivative in Eq. (13).

We employ the perturbed linear eikonal equation (38) to derive a control signal enforcing a desired shape while simultaneously preserving the one-dimensional wave profile $\mathbf{U}_c(\rho)$ along the coordinate ρ . One possible solution of the integral equation (38) for the control function is given by

$$\mathbf{f}(\boldsymbol{\chi}(\rho, s, t), t) = (c - c_n - \alpha \kappa) \mathcal{G}^{-1}(\mathbf{U}_c(\rho)) \mathbf{U}'_c(\rho). \quad (39)$$

Similar as in case of the nonlinear phase diffusion equation, we can also find another solution for \mathbf{f} which does not involve α ,

$$\mathbf{f}(\boldsymbol{\chi}(\rho, s, t), t) = \mathcal{G}^{-1}(\mathbf{U}_c(\rho)) (c - c_n - \mathcal{D}\kappa) \mathbf{U}'_c(\rho). \quad (40)$$

Again we obtain a control function without any reference to the response function \mathbf{W}^{\dagger} . Noteworthy, in order

to control a wave pattern with the proposed method, we solely need to know the velocity c , the invertible coupling matrix \mathcal{G} , the one-dimensional wave profile \mathbf{U}_c , and the matrix of diffusion coefficients \mathcal{D} .

Numerical simulations are typically performed in Cartesian coordinates $\mathbf{r} = (x, y)^T$. To evaluate the control function Eq. (40), we need to express $(\rho, s)^T$ in terms of the Cartesian coordinates $(x, y)^T$. Thus we have to invert the coordinate transform Eq. (33) for every time step. In general, this can only be done numerically, with the Newton-Raphson root finding method as a possible algorithm.

Below, we present a specific example. We choose a parametrization of the curve in polar coordinates

$$\boldsymbol{\gamma}(s, t) = R(s, t) \begin{pmatrix} \cos(s) \\ \sin(s) \end{pmatrix}, \quad (41)$$

whereby the coordinate s is restricted to $0 \leq s < 2\pi$. The normal vector $\mathbf{n}(s, t)$ and normal velocity c_n of the curve are given by

$$\mathbf{n}(s, t) = \frac{\begin{pmatrix} \cos(s) R'(s, t) - \sin(s) R(s, t) \\ \cos(s) R(s, t) + \sin(s) R'(s, t) \end{pmatrix}}{\sqrt{R(s, t)^2 + (R'(s, t))^2}}, \quad (42)$$

and

$$\begin{aligned} c_n(s, t) &= \mathbf{n}(s, t) \cdot \dot{\boldsymbol{\gamma}}(s, t) \\ &= \frac{R(s, t) \dot{R}(s, t)}{\sqrt{R(s, t)^2 + (R'(s, t))^2}}, \end{aligned} \quad (43)$$

respectively. For the curvature κ follows

$$\kappa(s, t) = \frac{R(s, t)^2 + 2(R'(s, t))^2 - R(s, t)R''(s, t)}{(R(s, t)^2 + (R'(s, t))^2)^{3/2}}. \quad (44)$$

To find the new coordinates $(\rho, s)^T$ in terms of the Cartesian coordinates $\mathbf{r} = (x, y)^T$, we proceed as follows. At the curve $\boldsymbol{\chi}(0, s, t) = \boldsymbol{\gamma}(s, t)$, the coordinate transform Eq. (33) can be inverted and the coordinate s is given by

$$s = \arctan(x, y). \quad (45)$$

The two-argument function $\arctan(x, y)$ denotes the arctangent of y/x within the range $(-\pi, \pi]$ instead of $(-\pi/2, \pi/2)$ as given for the usual $\arctan(y/x)$. Close to the curve $\boldsymbol{\chi}(0, s, t) = \boldsymbol{\gamma}(s, t)$, we can expand $\boldsymbol{\chi}(\rho, s, t)$ around $(\rho_0, s_0)^T$ with $\rho_0 = 0$

$$\begin{aligned} \boldsymbol{\chi}(\rho, s, t) &\approx \boldsymbol{\chi}(\rho_0, s_0, t) + J(\rho_0, s_0) \cdot \begin{pmatrix} \rho - \rho_0 \\ s - s_0 \end{pmatrix} \\ &= \boldsymbol{\gamma}(s_0, t) + J(0, s_0) \cdot \begin{pmatrix} \rho \\ s - s_0 \end{pmatrix}, \end{aligned} \quad (46)$$

where $J(\rho, s)$ denotes the Jacobian of the coordinate transformation Eq. (33). Solving this linear equation, we find

$$\begin{pmatrix} \rho \\ s \end{pmatrix} = \begin{pmatrix} 0 \\ s_0 \end{pmatrix} + J^{-1}(0, s_0) \cdot (\mathbf{r} - \boldsymbol{\gamma}(s_0, t)) \quad (47)$$

with s_0 given by $s_0 = \arctan(x, y)$. This approximation is valid close to the curve $\boldsymbol{\gamma}$ but deteriorates further away from it. Thus, for better accuracy, we apply the Newton-Raphson iteration

$$\begin{pmatrix} \rho_{k+1} \\ s_{k+1} \end{pmatrix} = \begin{pmatrix} \rho_k \\ s_k \end{pmatrix} + J^{-1}(\rho_k, s_k) \cdot (\mathbf{r} - \boldsymbol{\gamma}(s_k, t)), \quad (48)$$

with the initial values

$$\rho_0 = 0, \quad s_0 = \arctan(x, y). \quad (49)$$

In numerical simulations we perform typically 100 iterations of Eq. (48) to achieve a sufficiently accurate result. In the following, we apply the shape control Eq. (40) to the FitzHugh-Nagumo (FHN) model [42, 43]

$$\begin{aligned} \partial_t u &= D_u \Delta u + 3u - u^3 - v + \epsilon(\mathcal{G}_{11} f_u + \mathcal{G}_{12} f_v), \\ \partial_t v &= D_v \Delta v + \tilde{c}(u - \delta) - \tilde{c}\gamma v + \epsilon(\mathcal{G}_{21} f_u + \mathcal{G}_{22} f_v). \end{aligned} \quad (50)$$

In the absence of control, equations (50) possess a well known stable traveling pulse solution in one spatial dimension. No exact analytical expression is known for this solution. Therefore, we use a numerically determined, linearly interpolated one-dimensional pulse profile to evaluate $\mathbf{U}'_c(\rho)$ in the control signal Eq. (40). \mathcal{G}_{ij} denotes the components of the coupling matrix \mathcal{G} which we set to $\mathcal{G} = \mathbf{1}$ for simplicity. We initialize the controlled pattern sufficiently far away from any domain boundary so that the Neumann boundary conditions Eq. (2) are approximately satisfied. The parameters for the FHN model are

$$\tilde{c} = 0.33, \delta = -1.3, \gamma = 0, D_u = 1.0, D_v = 0.3. \quad (51)$$

Without control, an initially circular wave pattern propagates radially outwards with a time dependent radius $r(t) = 1/\kappa(t)$ given by the solution of the unperturbed linear eikonal equation (37),

$$\dot{r}(t) = c - \frac{\alpha}{r(t)}, \quad (52)$$

as

$$\begin{aligned} r(t) &= \frac{\alpha}{c} w \left(\left(\frac{cR_0}{\alpha} - 1 \right) \exp \left(\frac{c}{\alpha} (c(t - t_0) + R_0) - 1 \right) \right) \\ &\quad + \frac{\alpha}{c}. \end{aligned} \quad (53)$$

Here, R_0 is the initial radius and $w(z)$ denotes the Lambert w function. We design a control which impedes outward propagation and deforms the circular pattern into a flower-like shape with 5 petals. For that purpose we set

$$R(s, t) = R_0 + \frac{At}{T} \cos(ms) \quad (54)$$

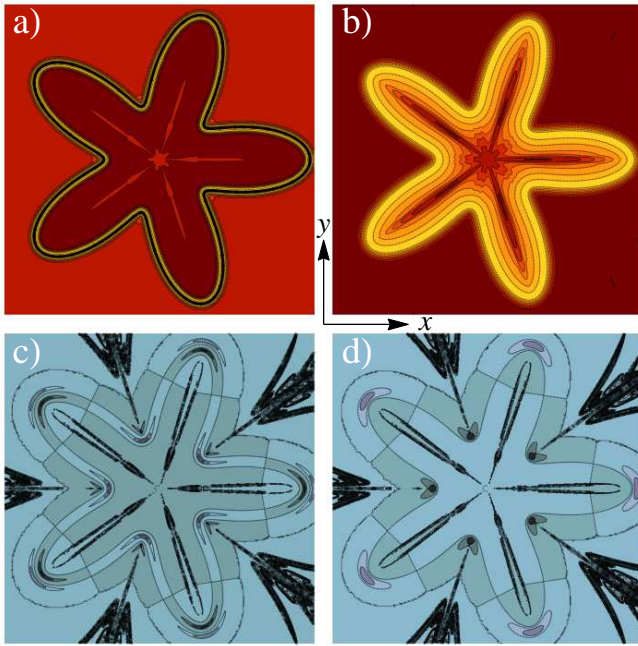


Figure 3. (Color online) Shaping a circular FitzHugh-Nagumo pulse to a flower with five petals. a) activator u , b) inhibitor v , c) activator control f_u , d) inhibitor control f_v . The protocol curve $\gamma(s, t)$ outlining the maximum activator value is shown as the black line (top left). Small numerical artifacts resulting from inverting the coordinate transform χ from Cartesian (x, y) to local coordinates (ρ, s) can be seen as a dark shadow in the control functions. Domain size is $L_x = L_y = 150$. See Supplemental Material [38] for a movie.

with

$$R_0 = 50, \quad A = 40, \quad m = 5, \quad T = 5. \quad (55)$$

Fig. 3 shows a snapshot of the time evolution under this control, see the Supplemental Material [38] for a movie. The control deforms the activator, Fig. 3a), and the inhibitor shape, Fig. 3b), into a flower like pattern. The position of the traveling wave, given by the maximum activator value, follows the prescribed curve γ (black solid line in Fig. 3a)) closely. Fig. 3c) and Fig. 3d) display the corresponding control functions f_u and f_v , respectively. The control signals attain its largest amplitudes at the points of largest curvature κ along the curve γ . Small numerical noise is visible as a dark shadow and results from the imperfect inversion of the coordinate transform via the Newton-Raphson algorithm Eq. (48).

V. POSITION CONTROL IN FINITE DOMAINS

Strictly speaking, traveling wave solutions with stationary profile \mathbf{U}_c in a comoving frame can only be defined in an infinite domain. Any terms in the RD system, including boundary conditions, which break the translational invariance of the system, destroy the existence of a

traveling wave solution \mathbf{U}_c . However, numerical computations of RD systems on finite domains Ω often assume homogeneous Neumann boundary conditions

$$\hat{\mathbf{N}}(\mathbf{r}) \cdot \nabla \mathbf{u}(\mathbf{r}, t) = 0, \quad \mathbf{r} \in \Gamma = \partial\Omega, \quad (56)$$

where Γ denotes the domain boundary, $\hat{\mathbf{N}}$ is the unit vector normal to the domain boundary, and the gradient ∇ acts component-wise on the vector \mathbf{u} . Physically, Neumann boundary conditions describe a vanishing flux of components \mathbf{u} across the boundary. Traveling wave solutions to RD systems are typically localized in the sense that the derivatives of any order $n \geq 1$ of the wave profile $\mathbf{U}_c(\xi)$ with respect to the traveling wave coordinate ξ decay to zero,

$$\lim_{\xi \rightarrow \pm\infty} \partial_\xi^n \mathbf{U}_c(\xi) = 0. \quad (57)$$

Because of the localization Eq. (57), the Neumann boundary conditions are approximately satisfied if the position of traveling waves is sufficiently far away from the boundaries such that the wave pattern is unaffected by the Neumann boundary. Sufficiently close to a Neumann boundary, the wave interacts with the boundary, and our proposed bulk control functions \mathbf{f} , acting inside the domain Ω , might fail because it was derived under the assumption of an unbounded domain. In this section we show that this is indeed the case, and demonstrate that the application of an additional boundary control successfully restores position control of traveling waves. Assuming that the in- or outflux \mathbf{b} of components across the boundary can be controlled, we introduce an inhomogeneous Neumann boundary condition with a boundary control term $\mathbf{b}(\mathbf{r}, t)$ as inhomogeneity,

$$\hat{\mathbf{N}}(\mathbf{r}) \cdot \nabla \mathbf{u}(\mathbf{r}, t) = \mathbf{b}(\mathbf{r}, t), \quad \mathbf{r} \in \Gamma. \quad (58)$$

Enforcing a desired distribution inside the domain solely by the boundary control \mathbf{b} is important for applications and can be achieved by optimal control, see e.g. [44] for an example and [22, 45] for the general approach. However, here we assume that additionally to the bulk control signal $\mathbf{f}(x, t)$ inside the domain Ω a control \mathbf{b} acts on the domain boundary.

For simplicity we consider a one-dimensional RD system. A generalization to higher spatial dimensions is straightforward. Due to the finite spatial domain the traveling wave profile $\mathbf{U}_c(x - ct)$ ceases to be a solution of the unperturbed RD system Eq. (1) with $\epsilon = 0$. However, it becomes again an exact solution if we supplement the RD system with the inhomogeneous Neumann boundary condition

$$\partial_x \mathbf{u}(x, t) = \mathbf{U}'_c(x - ct), \quad x \in \Gamma. \quad (59)$$

These considerations lead to a generalization of position control for traveling waves in finite domains. The controlled system now reads, with $\epsilon = 1$ as before,

$$\partial_t \mathbf{u}(x, t) = \mathcal{D} \partial_x^2 \mathbf{u} + \mathbf{R}(\mathbf{u}) + \epsilon \mathbf{f}(x, t), \quad x \in \Omega \subset \mathbb{R} \quad (60)$$

$$\partial_x \mathbf{u}(x, t) = \mathbf{U}'_c(x - ct) + \epsilon \mathbf{b}(x, t), \quad x \in \Gamma. \quad (61)$$

The bulk control follows from the one-dimensional version of Eq. (28) and Eq. (40), see also [20],

$$\mathbf{f}(x, t) = \left(c - \dot{\phi}(t) \right) \mathbf{U}'_c(x - \phi(t)), \quad (62)$$

while the boundary control is given by

$$\mathbf{b}(x, t) = \mathbf{U}'_c(x - \phi(t)) - \mathbf{U}'_c(x - ct), \quad x \in \Gamma. \quad (63)$$

This yields the inhomogeneous Neumann boundary condition intuitively expected for a traveling wave shifted according to the protocol:

$$\partial_x \mathbf{u}(x, t) = \mathbf{U}'_c(x - \phi(t)), \quad x \in \Gamma. \quad (64)$$

Fig. (4) proves the need for boundary control in the case of the one-dimensional Schlögl model, Eq. (29) in one spatial dimension. The task is to move the front across the boundary according to the protocol

$$\begin{aligned} \phi(t) = & \phi_0 + \Theta(t_1 - t) \frac{c(t_1 - t_0)}{\pi} \sin\left(\pi \frac{t - t_0}{t_1 - t_0}\right) \\ & - c(t - t_1) \Theta(t - t_1), \end{aligned} \quad (65)$$

where Θ denotes the Heaviside step function. Bulk as well as boundary control are switched on at $t = t_0$ upon which the unperturbed front moves with velocity c . The protocol smoothly reverses the propagation direction at a time instant when the front is located outside the domain. After the time $t = t_1$, the front moves backwards with velocity $-c$. For numerical simulations we set $\phi_0 = 63.28$, $t_1 - t_0 = 15$, and $L = 60$ for the domain size. The white line in the top panel of Fig. 4 shows a space-time plot of the position of the traveling wave determined by $u(x, t) = 1/2$. In Fig. 4 left, only the bulk control Eq. (62) is applied. A front which has moved beyond the domain boundary cannot be forced back into the domain. On the contrary, under both bulk and boundary control the front can successfully be returned, see Fig. 4 right. The top panels show the spatio-temporal bulk control $\mathbf{f}(x, t)$ (gray) and a contour of the Schlögl front (white), while the bottom panels show the boundary control b over time, i.e., Eq. (63) evaluated at the domain boundary $x = L$.

VI. CONCLUSIONS

We have presented a method to control the shape of two-dimensional traveling waves in RD systems. The desired wave shape is prescribed by a time-dependent curve γ . An inverse problem for the determination of the control signal \mathbf{f} that forces the wave to adopt the shape outlined by γ is formulated in terms of well-known evolution equations for wave patterns, namely the linear eikonal equation and the nonlinear phase diffusion equation. The feasibility of the proposed approach is demonstrated by numerical simulations of simple but representative examples of controlled RD systems.

Two variants of this control method with different areas

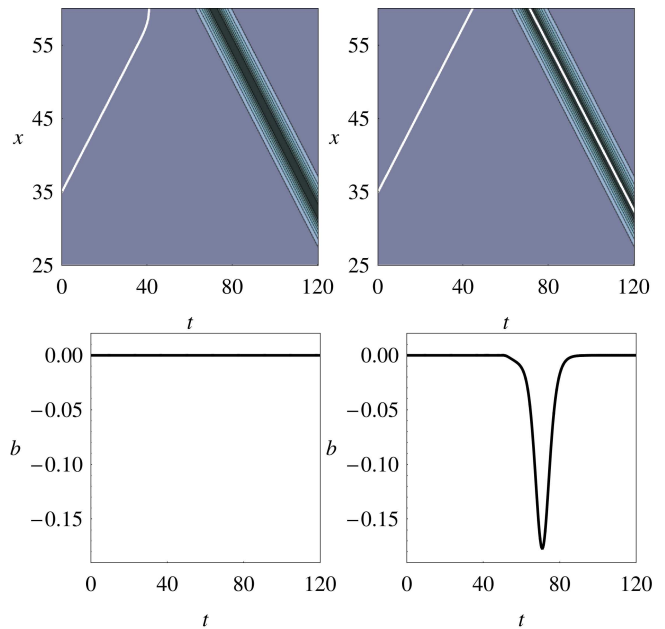


Figure 4. (Color online) Additionally to the bulk control $\mathbf{f}(x, t)$ acting inside the domain, a boundary control $b(t)$ is necessary to move a wave from inside the domain to the outside and back again. Top: Space-time plot of the bulk control $\mathbf{f}(x, t)$ acting inside the domain. Light (dark) corresponds to a high (low) value of \mathbf{f} . The white line denotes the contour of the Schlögl front with $u(x, t) = 1/2$. Bottom: Boundary control over time applied at the upper domain boundary at $x = 60$. Left: Under bulk control alone, a front leaving the domain cannot be returned. Right: With additional boundary control the front is successfully forced back into the domain. Parameter of the Schlögl model is $a = 0.1$. See Supplemental Material [38] for two movies.

of application are presented. The first one is suited to shape wave patterns close to plane waves. In this case the control signal, Eq. (28), is given as the solution of an integral equation based on the perturbed nonlinear phase diffusion equation (13). The corresponding desired concentration fields enforced by the control are

$$\mathbf{u}_d(\mathbf{r}, t) = \mathbf{U}_c(x - \phi(y, t)), \quad (66)$$

where \mathbf{U}_c is the uncontrolled one-dimensional wave profile and $\phi(y, t)$ denotes the x -component of the curve $\gamma(y, t) = (\phi(y, t), y)^T$ outlining the wave shape. Because γ is parametrized in Cartesian coordinates, the control signal \mathbf{f} , Eq. (28), can be readily evaluated.

The second control method allows to enforce a wave shape described by a curve γ which is not necessarily close to a plane wave but has a sufficiently small curvature such that the linear eikonal equation (37) is valid. The control signal Eq. (40) is obtained from the perturbed eikonal equation (38) which is interpreted as an integral equation for the unknown control \mathbf{f} enforcing a wave shape γ specified in advance. The corresponding

desired concentration fields are

$$\mathbf{u}_d(\mathbf{r}, t) = \mathbf{U}_c(\rho), \quad (67)$$

with $\rho = \rho(\mathbf{r}, t)$ given by the inverse of the coordinate transformation Eq. (33). To evaluate the control signal $\mathbf{f}(\boldsymbol{\chi}(\rho, s, t), t)$, this inverse coordinate transformation must be computed for every time step. This renders the second control method computationally much more expensive than the first.

In principle one could quantify the performance of a certain control signal by evaluating the squared difference between the desired concentration fields \mathbf{u}_d , Eq. (66) or Eq. (67), and the actual numerical result \mathbf{u} of the controlled RD system and integrate the result over the spatiotemporal computational domain $[0, L_x] \times [0, L_y] \subset \mathbb{R}^2$,

$$S = \frac{1}{(t_1 - t_0) L_x L_y} \int_{t_0}^{t_1} dt \int_0^{L_x} dx \int_0^{L_y} dy (\mathbf{u}(\mathbf{r}, t) - \mathbf{u}_d(\mathbf{r}, t))^2. \quad (68)$$

A constrained functional as in Eq. (68) would also be the starting point for an optimal control algorithm, i.e., an iterative algorithm which aims to minimize S [21–23].

We emphasize that the control signal \mathbf{f} is always expressed solely in terms of the derivative $\mathbf{U}'_c(\xi)$ of the uncontrolled one-dimensional traveling wave profile, its propagation velocity c , the diagonal matrix of diffusion coefficients \mathcal{D} and the invertible coupling matrix \mathcal{G} . We are able to eliminate any reference to the response function $\mathbf{W}^\dagger(x)$ and consequently, to apply our method it is not necessary to know the reaction kinetics \mathbf{R} . This makes the approach useful for applications where the underlying reaction kinetics is not at all or only approximately known, while in the absence of control, the traveling wave profile \mathbf{U}_c of all state variables and its propagation velocity c can be measured with sufficient accuracy. In case that only an incomplete number of (combinations of) state variables can be measured, observer techniques from nonlinear control theory [46, 47] or other state estimation and fitting procedures can be applied to reconstruct the complete state. However, this usually requires a more detailed knowledge of the reaction kinetics. In contrast to feedback control, which necessitates the continuous estimation of the complete state of the actual system to be controlled, for our approach it is sufficient to obtain the wave profile of all state variables from an identical copy of the uncontrolled system. Therefore, a much larger variety of measurement techniques, as e.g. destructive measurements, can be deployed, and the notion of nonlinear state observability [48] developed for feedback control does not apply in our case. Once the wave profile \mathbf{U}_c is obtained with sufficient accuracy, the application of our control scheme merely requires the knowledge of the initial shape of the wave pattern to be controlled, which can be obtained from the measurement of a single state component.

In the derivation of the perturbed eikonal and phase diffusion equations, Eq. (38) and Eq. (13), respectively, we

assumed a small amplitude of the control signal \mathbf{f} . Note that the control amplitude $c - c_n - \alpha\kappa$ in Eq. (39) is zero if and only if the time evolution of the curve γ is governed by the unperturbed linear eikonal equation (37). In other words, trying to enforce a wave shape which is a solution of the unperturbed RD equations leads to a vanishing control signal \mathbf{f} .

In the examples discussed so far the coupling matrix is restricted to the simplest possible case $\mathcal{G} = \mathbf{1}$. However, our method can be readily generalized to more complex but invertible coupling matrices. For multi-component systems, invertibility of \mathcal{G} implies that the number m of independent control signals $\mathbf{f}(\mathbf{r}, t) = (f_1(\mathbf{r}, t), \dots, f_m(\mathbf{r}, t))$ is equal to the number n of components $\mathbf{u}(\mathbf{r}, t) = (u_1(\mathbf{r}, t), \dots, u_n(\mathbf{r}, t))^T$ of the RD system. Using the control solution $\mathbf{f}(\mathbf{r}, t) = (f_u(\mathbf{r}, t), f_v(\mathbf{r}, t))^T$, Eq. (40), for the controlled Fitz-Hugh Nagumo model, Eq. (50), with $\mathcal{G} = \mathbf{1}$, we demonstrate how the method can be generalized if the coupling matrix \mathcal{G} is not invertible and the control \tilde{f}_u is acting solely on the activator variable,

$$\begin{aligned} \partial_t u &= D_u \Delta u + 3u - u^3 - v + \epsilon \tilde{f}_u, \\ \partial_t v &= D_v \Delta v + \tilde{\epsilon}(u - \delta) - \tilde{\epsilon} \gamma v. \end{aligned} \quad (69)$$

The FitzHugh-Nagumo model Eq. (50) with $\mathcal{G} = \mathbf{1}$ can be written as a single nonlinear integrodifferential equation for the activator u ,

$$\begin{aligned} \partial_t u &= D_u \Delta u + 3u - u^3 - \mathcal{K}(\tilde{\epsilon}(u - \delta) + \epsilon f_v) \\ &\quad - \mathcal{K}_0 v_0 + \epsilon f_u. \end{aligned} \quad (70)$$

Here, \mathcal{K} and \mathcal{K}_0 are integral operators, involving Green's function, of the inhomogeneous linear PDE for the inhibitor v with initial condition $v(\mathbf{r}, t_0) = v_0(\mathbf{r})$,

$$\partial_t v - D_v \Delta v + \tilde{\epsilon} \gamma v = \tilde{\epsilon}(u - \delta) + \epsilon f_v. \quad (71)$$

Equation (69) can be written as single nonlinear integrodifferential equation as well. Comparing the control terms of both integrodifferential equations, we obtain a solution for the control \tilde{f}_u as

$$\tilde{f}_u(\mathbf{r}, t) = -\mathcal{K} f_v(\mathbf{r}, t) + f_u(\mathbf{r}, t). \quad (72)$$

The term $h(\mathbf{r}, t) = \mathcal{K} f_v(\mathbf{r}, t)$ can be computed as the solution to the inhomogeneous PDE

$$\partial_t h - D_v \Delta h + \tilde{\epsilon} \gamma h = f_v(\mathbf{r}, t) \quad (73)$$

with initial condition $h(\mathbf{r}, t_0) = 0$. This computation requires more knowledge of the underlying reaction kinetics when compared to the case of an invertible coupling matrices, namely the values of the parameters $\tilde{\epsilon}$ and γ must be known. See [20] and the accompanying supplement for one-dimensional numerical simulations of the controlled RD system with singular coupling matrix, Eq. (69), and a comparison with optimal control as well as a generalization to Hodgkin-Huxley type and other RD models. An important aspect of the proposed control method is

stability. Stability means that the controlled reaction-diffusion system (1) must yield a solution which is sufficiently close to the desired distribution, Eq. (66) or Eq. (67). For position control of traveling waves in one spatial dimension, the controlled reaction-diffusion system (1) with control function Eq. (62),

$$\begin{aligned} \partial_t \mathbf{u} = \mathcal{D} \partial_x^2 \mathbf{u} + \mathbf{R}(\mathbf{u}) + \left(c - \dot{\theta}(t) \right) \mathbf{U}'_c(x - \theta(t)) \\ + \hat{\epsilon} \mathbf{q}(\mathbf{u}, x, t), \end{aligned} \quad (74)$$

must be stable against structural perturbations $\mathbf{q}(\mathbf{u}, x, t)$ of the system equations itself as well as stable against perturbations \mathbf{z}_0 and ΔX of the initial conditions,

$$\mathbf{u}(x, t_0) = \mathbf{U}_c(x - \theta_0 - \Delta X) + \hat{\epsilon} \mathbf{z}_0(x). \quad (75)$$

The latter arise if e.g. the initial condition is not exactly the traveling wave solution \mathbf{U}_c , or if the control is applied initially at a position $\theta_0 = \theta(t_0)$ different from the actual initial position $\theta_0 + \Delta X$ of the traveling wave to be controlled. Structural perturbations \mathbf{q} could be spatial heterogeneities of the reaction-diffusion medium, for example, or errors in measurements of the traveling wave profile \mathbf{U}_c which cause an incorrect and noisy control function. For a quantitative analysis, the parameter $\hat{\epsilon} \ll 1$ is assumed to be small such that the system can be linearized with an appropriate ansatz. Note that $\hat{\epsilon}$ is not necessarily of the same magnitude as the original small parameter ϵ in Eq. (1), which we set to $\epsilon = 1$ here. The solution \mathbf{v} to the linear equations can be written as a superposition of eigenfunctions \mathbf{v}_i of the linear operator \mathcal{L} , Eq. (4), weighted by factors $\sim \exp(-\lambda_i t)$ [20], where λ_i is the i -th eigenvalue of \mathcal{L} . If the traveling wave solution \mathbf{U}_c is stable and exhibits a spectral gap, then all eigenvalues for $i > 0$ have a real part $\Re(\lambda_i) < 0$. Therefore, apart from the Goldstone mode $\mathbf{v}_0 = \mathbf{W} = \mathbf{U}'_c$ corresponding to the zero eigenvalue $\lambda_0 = 0$, any perturbation $\hat{\epsilon} \mathbf{z}_0$ of the initial conditions decays to zero for large times. The larger is the spectral gap, the faster decays the perturbation. Similarly, any structural perturbation $\hat{\epsilon} \mathbf{q}(\mathbf{u}, x, t)$ decays to a term with magnitude proportional to $\hat{\epsilon}$, leading merely to a small time-dependent deformation of the traveling wave profile \mathbf{U}_c as long as $\hat{\epsilon}$ is sufficiently small. Because the Goldstone mode with eigenvalue $\lambda_0 = 0$ does not decay in time, it requires special treatment. In [24], we derived and analyzed an EOM very similar to Eq. (18) which takes into account the dynamics of the Goldstone mode. This analysis established the stability of position control against perturbations ΔX of the initial position in the absence of structural perturbations. In accordance with numerical simulations, we found that an interval of perturbations ΔX exists for which position control is stable. The size of this interval is a measure for the stability against perturbations of the initial position, and, in general, depends on the reaction kinetics in a complicated way. The interval vanishes for stationary traveling waves with reflection symmetry. As for the effect of structural perturbations $\mathbf{q}(\mathbf{u}, x, t)$, we expect that as long as the

parameter $\hat{\epsilon}$ characterizing the amplitude of structural perturbations is sufficiently small, this interval does still exist. In principle, structural perturbations cannot only shrink the interval but also enlarge it, thereby exerting a destabilizing or stabilizing influence on position control, respectively. Going from one to two spatial dimensions, new phenomena as e.g. transversal instabilities arise [2, 4] which can destabilize an uncontrolled plane wave. However, we expect that our qualitative discussion of stability also applies in this case provided a plane wave is stable and exhibits a spectral gap. A rigorous quantitative justification of the arguments above is quite involved and set aside for future publications.

Generalizations of the linear eikonal equation and the nonlinear phase diffusion equation to three spatial dimensions describe the evolution of isoconcentration surfaces. We expect that along the lines of the approach discussed in the present paper it will be possible to control the shape of three-dimensional wave patterns in RD systems.

In view of the growing relevance of RD models in such diverse fields as (bio-)chemical reactions, population dynamics [49], the cooperative self-organization of microorganisms [50], infectious diseases [51], and physiology [52], imaginable applications for our proposed control method abound. We mention the prevention of the spreading of epidemics [53], guiding of chemically propelled nanomotors interacting with chemical waves [54, 55], the growth of crystals into desired shapes [56, 57], and the control of evolving cell cultures as e.g. tumor progression [58, 59]. Possible experimental systems to test the feasibility of the proposed control method are the light-sensitive BZ reaction [8] or a liquid crystal light valve with optical feedback [60–62], see also the discussion in [63].

Appendix A: Derivation of the perturbed nonlinear phase diffusion equation

We start with the perturbed RD system

$$\partial_t \mathbf{u} = \mathcal{D} \Delta \mathbf{u} + \mathbf{R}(\mathbf{u}) + \epsilon \mathbf{f}(\mathbf{u}, x, y, t), \quad (\text{A1})$$

where $\Delta = \partial_x^2 + \partial_y^2$ is the Laplacian and \mathcal{D} is a diagonal matrix of constant diffusion coefficients. The space domain extends from $-\infty$ to ∞ in the x -direction. In the y -direction it is either finite with no flux or periodic boundary conditions, or infinite as well. The goal is to derive an equation for the shape $\phi(y, t)$ of the wave over time. The unperturbed solution is assumed to be a traveling wave $\mathbf{U}_c(x - ct)$ propagating with constant velocity c in the x -direction. The wave profile is stationary in the comoving frame with $\xi = x - ct$, i.e., \mathbf{U}_c obeys

$$\mathcal{D} \mathbf{U}_c''(\xi) + c \mathbf{U}_c'(\xi) + \mathbf{R}(\mathbf{U}_c(\xi)) = 0. \quad (\text{A2})$$

We introduce a slow time scale, $T = \epsilon t$, and a stretched spatial coordinate in the y -direction, $Y = \epsilon^{1/2} y$. Bearing

in mind the replacements

$$\partial_t \rightarrow \partial_t + \partial_t T \partial_T = \partial_t + \epsilon \partial_T, \quad (\text{A3})$$

$$\partial_y \rightarrow \partial_y + \partial_y Y \partial_Y = \partial_y + \epsilon^{1/2} \partial_Y, \quad (\text{A4})$$

$$\partial_y^2 \rightarrow \left(\partial_y + \epsilon^{1/2} \partial_Y \right) \left(\partial_y + \epsilon^{1/2} \partial_Y \right) = \partial_y^2 + 2\epsilon^{1/2} \partial_y \partial_Y + \epsilon \partial_Y^2, \quad (\text{A5})$$

and the ansatz for the solution

$$\mathbf{u}(x, y, t, Y, T) = \mathbf{U}_c(x - ct + p(Y, T)) + \epsilon \mathbf{v}(x - ct + p(Y, T), y, t, Y, T), \quad (\text{A6})$$

we derive a PDE for $p(Y, T)$. We get

$$\begin{aligned} \partial_t \mathbf{u} + \epsilon \partial_T \mathbf{u} &= \mathcal{D} \Delta \mathbf{u} + 2\mathcal{D} \epsilon^{1/2} \partial_y \partial_Y \mathbf{u} \\ &+ \epsilon \mathcal{D} \partial_Y^2 \mathbf{u} + \mathbf{R}(\mathbf{u}) + \epsilon \mathbf{f}(\mathbf{u}, x, y, t), \end{aligned} \quad (\text{A7})$$

and for the derivatives in y -direction up to $\mathcal{O}(\epsilon)$

$$\epsilon^{1/2} \partial_y \partial_Y \mathbf{u} = \epsilon^{1/2} \partial_Y \partial_y \mathbf{u} = 0 + \mathcal{O}(\epsilon^{3/2}). \quad (\text{A8})$$

Expanding Eq. (A7) with the ansatz Eq. (A6) up to $\mathcal{O}(\epsilon^{3/2})$ yields

$$\begin{aligned} \epsilon \mathbf{U}'_c \partial_T p + \epsilon \partial_t \mathbf{v} &= \mathcal{D} \mathbf{U}''_c + c \mathbf{U}'_c + \mathbf{R}(\mathbf{U}_c) \\ &+ \epsilon \mathcal{D} \mathbf{U}''_c (\partial_Y p)^2 + \epsilon \mathcal{D} \mathbf{U}'_c \partial_Y^2 p + \epsilon \mathcal{D} \Delta \mathbf{v} \\ &+ \epsilon c \partial_\xi \mathbf{v} + \epsilon \mathbb{D} \mathbf{R}(\mathbf{U}_c) \mathbf{v} + \epsilon \mathbf{f} + \mathcal{O}(\epsilon^{3/2}). \end{aligned} \quad (\text{A9})$$

Here, $\mathbb{D} \mathbf{R}(\mathbf{U}_c)$ denotes the Jacobian of \mathbf{R} and we have transformed to the comoving coordinate $\xi = x - ct$. The control reads now

$$\mathbf{f} = \mathbf{f}(\mathbf{U}_c(\xi + p(Y, T)), \xi + ct, y, t) + \mathcal{O}(\epsilon). \quad (\text{A10})$$

Simplifying leads to the following equation in order $\mathcal{O}(\epsilon)$

$$\mathbf{U}'_c \partial_T p = \mathcal{D} \mathbf{U}''_c (\partial_Y p)^2 + \mathcal{D} \mathbf{U}'_c \partial_Y^2 p - \partial_t \mathbf{v} + \mathcal{L} \mathbf{v} + \mathbf{f}, \quad (\text{A11})$$

where we have introduced

$$\mathcal{L} = \mathcal{D} (\partial_\xi^2 + \partial_y^2) + c \partial_\xi + \mathbb{D} \mathbf{R}(\mathbf{U}_c(\xi + p(Y, T))). \quad (\text{A12})$$

The operator \mathcal{L} acts on the function $\mathbf{v} = \mathbf{v}(\xi + p(Y, T), y, Y, T)$. Now let us suppose we know the eigenfunction \mathbf{W}^\dagger to the eigenvalue zero of the operator \mathcal{L}^\dagger adjoint to \mathcal{L} with respect to the standard inner product in function space

$$\langle \mathbf{w}(\xi), \mathbf{v}(\xi) \rangle = \int_{-\infty}^{\infty} d\xi \mathbf{w}^T(\xi) \mathbf{v}(\xi), \quad (\text{A13})$$

where \mathbf{w}^T denotes the transpose of vector \mathbf{w} . $\mathbf{W}^\dagger = \mathbf{W}^\dagger(\xi + p(Y, T))$ is called the adjoint Goldstone

mode. In general, and particularly in higher spatial dimensions, there can be more than one adjoint Goldstone mode. The second contribution $\mathbf{v}(x - ct + p(Y, T), y, t, Y, T)$ of the ansatz Eq.(A6) involves a sum over all eigenfunctions of \mathcal{L} . However, the first contribution $\mathbf{U}_c(x - ct + p(Y, T))$ of Eq.(A6) includes already the effect of the Goldstone mode \mathbf{U}'_c because of $\mathbf{U}_c(\xi + p) \approx \mathbf{U}_c(\xi) + p \mathbf{U}'_c(\xi)$. Therefore, to exclude the Goldstone mode from \mathbf{v} , we have

$$\langle \mathbf{W}^\dagger, \mathbf{v} \rangle = 0, \quad (\text{A14})$$

from which follows

$$\langle \mathbf{W}^\dagger, \partial_t \mathbf{v} \rangle = 0 \quad (\text{A15})$$

because \mathbf{W}^\dagger is independent of t . So we find

$$\begin{aligned} -\langle \mathbf{W}^\dagger, \mathcal{L} \mathbf{v} \rangle &= -\langle \mathbf{W}^\dagger, \mathbf{U}'_c \rangle \partial_T p + \langle \mathbf{W}^\dagger, \mathcal{D} \mathbf{U}''_c \rangle (\partial_Y p)^2 \\ &+ \langle \mathbf{W}^\dagger, \mathcal{D} \mathbf{U}'_c \rangle \partial_Y^2 p + \langle \mathbf{W}^\dagger, \mathbf{f} \rangle. \end{aligned} \quad (\text{A16})$$

Eq. (A16) is also called a solvability condition or Fredholm alternative. Because of $\langle \mathbf{W}^\dagger, \mathcal{L} \mathbf{v} \rangle = \langle \mathcal{L}^\dagger \mathbf{W}^\dagger, \mathbf{v} \rangle = 0$, the right hand side must be zero, and we obtain the desired PDE for p as follows:

$$\begin{aligned} 0 &= -\langle \mathbf{W}^\dagger, \mathbf{U}'_c \rangle \partial_T p + \langle \mathbf{W}^\dagger, \mathcal{D} \mathbf{U}''_c \rangle (\partial_Y p)^2 \\ &+ \langle \mathbf{W}^\dagger, \mathcal{D} \mathbf{U}'_c \rangle \partial_Y^2 p + \langle \mathbf{W}^\dagger, \mathbf{f} \rangle. \end{aligned} \quad (\text{A17})$$

Note that with our ansatz for $\mathbf{v} = \mathbf{v}(\xi + p(T, Y), t, y, T, Y)$, we have

$$\begin{aligned} \langle \mathbf{W}^\dagger, \mathbf{v} \rangle &= \int_{-\infty}^{\infty} d\xi \mathbf{W}^{\dagger T}(\xi + p) \mathbf{v}(\xi + p, y, t, Y, T) \\ &= \int_{-\infty}^{\infty} d\xi \mathbf{W}^{\dagger T}(\xi) \mathbf{v}(\xi, y, t, Y, T) = 0, \end{aligned} \quad (\text{A18})$$

i.e., these inner products do not depend on p any more. An exception is the inner product involving the perturbation \mathbf{f} , which we transform back to an integral over original space \tilde{x} as follows,

$$\begin{aligned} \langle \mathbf{W}^\dagger, \mathbf{f} \rangle &= \int_{-\infty}^{\infty} d\xi \mathbf{W}^{\dagger T}(\xi + p) \mathbf{f}(\mathbf{U}_c(\xi + p), \xi + ct, y, t) \\ &= \int_{-\infty}^{\infty} d\tilde{x} \mathbf{W}^{\dagger T}(\tilde{x}) \mathbf{f}(\mathbf{U}_c(\tilde{x}), \tilde{x} + ct - p, y, t). \end{aligned} \quad (\text{A19})$$

In general,

$$\frac{\langle \mathbf{W}^\dagger, \mathcal{D} \mathbf{U}'_c \rangle}{\langle \mathbf{W}^\dagger, \mathbf{U}'_c \rangle} \neq \mathcal{D}, \quad (\text{A20})$$

since \mathcal{D} is a matrix of diffusion coefficients. Only if the diffusion coefficient is the same for all components, $\mathcal{D} = \mathcal{D} \mathbf{1}$, we have

$$\frac{\langle \mathbf{W}^\dagger, \mathcal{D} \mathbf{U}'_c \rangle}{\langle \mathbf{W}^\dagger, \mathbf{U}'_c \rangle} = \frac{\langle \mathbf{W}^\dagger, \mathcal{D} \mathbf{U}'_c \rangle}{\langle \mathbf{W}^\dagger, \mathbf{U}'_c \rangle} = \mathcal{D}. \quad (\text{A21})$$

We introduce a new function

$$\phi(y, t) = ct - p(Y, T) \quad (\text{A22})$$

with (see Eqs. (A3), (A5))

$$\partial_t \phi(y, t) = c - \epsilon \partial_T p(Y, T), \quad (\text{A23})$$

$$\partial_y \phi(y, t) = -\epsilon^{1/2} \partial_Y p(Y, T), \quad (\text{A24})$$

$$(\partial_y \phi(y, t))^2 = \epsilon (\partial_Y p(Y, T))^2, \quad (\text{A25})$$

$$\partial_y^2 \phi(y, t) = -\epsilon \partial_Y^2 p(Y, T), \quad (\text{A26})$$

and find

$$\begin{aligned} \partial_t \phi &= c - \epsilon \partial_T p \\ &= c - \frac{\langle \mathbf{W}^\dagger, \mathcal{D}\mathbf{U}_c'' \rangle}{\langle \mathbf{W}^\dagger, \mathbf{U}'_c \rangle} (\partial_y \phi)^2 + \frac{\langle \mathbf{W}^\dagger, \mathcal{D}\mathbf{U}_c' \rangle}{\langle \mathbf{W}^\dagger, \mathbf{U}'_c \rangle} \partial_y^2 \phi \\ &\quad - \epsilon \frac{\langle \mathbf{W}^\dagger, \mathbf{f} \rangle}{\langle \mathbf{W}^\dagger, \mathbf{U}'_c \rangle}. \end{aligned} \quad (\text{A27})$$

Neumann boundary conditions for $\mathbf{u}(x, y, t)$ in y -direction, Eq. (2), carry over to Neumann boundary conditions for $\phi(y, t)$. Now we exploit the identity

$$\frac{\langle \mathbf{W}^\dagger, \mathcal{D}\mathbf{U}_c'' \rangle}{\langle \mathbf{W}^\dagger, \mathbf{U}'_c \rangle} = -\frac{c}{2}. \quad (\text{A28})$$

which was proven by Kuramoto in Ref. [2]. Finally, we obtain the perturbed nonlinear phase diffusion equation

$$\dot{\phi} = c + \frac{c}{2} (\phi')^2 + \frac{\langle \mathbf{W}^\dagger, \mathcal{D}\mathbf{U}_c' \rangle}{\langle \mathbf{W}^\dagger, \mathbf{U}'_c \rangle} \phi'' - \epsilon \frac{\langle \mathbf{W}^\dagger, \mathbf{f} \rangle}{\langle \mathbf{W}^\dagger, \mathbf{U}'_c \rangle}, \quad (\text{A29})$$

with a perturbation given by

$$\begin{aligned} \langle \mathbf{W}^\dagger, \mathbf{f} \rangle &= \int_{-\infty}^{\infty} dx \mathbf{W}^{\dagger T}(x - \phi) \mathbf{f}(\mathbf{U}_c(x - \phi), x, y, t) \\ &= \int_{-\infty}^{\infty} dx \mathbf{W}^{\dagger T}(x) \mathbf{f}(\mathbf{U}_c(x), x + \phi, y, t), \end{aligned} \quad (\text{A30})$$

and the constants

$$\langle \mathbf{W}^\dagger, \mathbf{U}'_c \rangle = \int_{-\infty}^{\infty} dx \mathbf{W}^{\dagger T}(x) \mathbf{U}'_c(x), \quad (\text{A31})$$

$$\langle \mathbf{W}^\dagger, \mathbf{U}''_c \rangle = \int_{-\infty}^{\infty} dx \mathbf{W}^{\dagger T}(x) \mathbf{U}''_c(x). \quad (\text{A32})$$

Appendix B: From the perturbed linear eikonal equation to the perturbed nonlinear phase diffusion equation

We derive the perturbed nonlinear phase diffusion equation (13) from the perturbed linear eikonal equation (38). If we parametrize the curve γ according to

$$\gamma(y, t) = \begin{pmatrix} \phi(y, t) \\ y \end{pmatrix}, \quad (\text{B1})$$

the linear eikonal equation becomes

$$\frac{\dot{\phi}}{\sqrt{(\phi')^2 + 1}} = c + \alpha \frac{\phi''}{((\phi')^2 + 1)^{3/2}}. \quad (\text{B2})$$

The ansatz for ϕ is

$$\phi(y, t) = ct + \Phi(Y, T) \quad (\text{B3})$$

with a slow time scale $T = \epsilon t$ and a stretched space scale $Y = \epsilon^{1/2} y$. Using Eq. (B3) in Eq. (B2), we obtain

$$\frac{c + \epsilon \dot{\Phi}}{\sqrt{\epsilon (\Phi')^2 + 1}} = c + \alpha \epsilon \frac{\Phi''}{(\epsilon (\Phi')^2 + 1)^{3/2}}. \quad (\text{B4})$$

With $(1 + \epsilon a)^{-1/2} = 1 - \frac{a}{2}\epsilon + \mathcal{O}(\epsilon^2)$, we expand Eq. (B4) and get

$$c - \epsilon \frac{c}{2} (\Phi')^2 + \epsilon \dot{\Phi} + \mathcal{O}(\epsilon^2) = c + \alpha \epsilon \Phi'' + \mathcal{O}(\epsilon^2), \quad (\text{B5})$$

or, after some rearrangement,

$$\epsilon \dot{\Phi} = \epsilon \frac{c}{2} (\Phi')^2 + \alpha \epsilon \Phi'' + \mathcal{O}(\epsilon^2). \quad (\text{B6})$$

Scaling back to original coordinates t, y , and introducing the original function ϕ we recover the nonlinear phase diffusion equation,

$$\dot{\phi} = c + \frac{c}{2} (\phi')^2 + \alpha \phi''. \quad (\text{B7})$$

To treat the perturbation term $\mathbf{f}(\chi(\rho, s, t), t)$, we express χ as

$$\begin{aligned} \chi(\rho, y, t) &= \gamma(y, t) + \rho \mathbf{n}(y, t) \\ &= \begin{pmatrix} \phi + \rho (1 + (\phi')^2)^{-1/2} \\ y - \rho \phi' (1 + (\phi')^2)^{-1/2} \end{pmatrix} \\ &= \begin{pmatrix} ct + \Phi + \rho (1 + \epsilon (\Phi')^2)^{-1/2} \\ y - \sqrt{\epsilon} \rho \Phi' (1 + \epsilon (\Phi')^2)^{-1/2} \end{pmatrix} \\ &= \begin{pmatrix} ct + \Phi + \rho \\ y \end{pmatrix} + \mathcal{O}(\sqrt{\epsilon}), \end{aligned} \quad (\text{B8})$$

such that finally

$$\chi(\rho, y, t) = \begin{pmatrix} \rho \\ y \end{pmatrix} + \phi \mathbf{e}_x + \mathcal{O}(\sqrt{\epsilon}). \quad (\text{B9})$$

The expansion can be truncated after the lowest order in ϵ because the perturbation \mathbf{f} is also multiplied by ϵ . Finally we get

$$\epsilon \int_{-\infty}^{\infty} d\rho \mathbf{W}^{\dagger T}(\rho) \mathcal{G}(\mathbf{U}_c(\rho)) \mathbf{f}(\chi(\rho, s, t), t)$$

$$\begin{aligned}
&= \epsilon \int_{-\infty}^{\infty} d\rho \mathbf{W}^{\dagger T}(\rho) \mathcal{G}(\mathbf{U}_c(\rho)) \mathbf{f} \left(\begin{pmatrix} \rho \\ y \end{pmatrix} + \phi \mathbf{e}_x, t \right) + \mathcal{O}(\epsilon^{3/2}) \\
&= \epsilon \int_{-\infty}^{\infty} dx \mathbf{W}^{\dagger T}(x) \mathcal{G}(\mathbf{U}_c(x)) \mathbf{f}(\mathbf{r} + \phi \mathbf{e}_x, t) + \mathcal{O}(\epsilon^{3/2}),
\end{aligned}
\tag{B10}$$

which is exactly the perturbation term in the nonlinear phase diffusion equation (13).

ACKNOWLEDGMENTS

We acknowledge financial support from the German Science Foundation (DFG) within the GRK 1558 (J. L.) and within the framework of the Collaborative Research Center 910 (S. M. and H. E.).

-
- [1] L. M. Pismen, *Patterns and interfaces in dissipative dynamics* (Springer, Berlin, 2006).
- [2] Y. Kuramoto, *Prog. Theor. Phys.* **63**, 1885 (1980).
- [3] V. S. Zykov, *Simulation of wave processes in excitable media* (Manchester University Press, Manchester, 1987).
- [4] Y. Kuramoto, *Chemical oscillations, waves, and turbulence* (Dover, New York, 2003).
- [5] H. Dierckx, O. Bernus, and H. Vershelde, *Phys. Rev. Lett.* **107**, 108101 (2011).
- [6] A. S. Mikhailov and K. Showalter, *Phys. Rep.* **425**, 79 (2006).
- [7] V. Vanag and I. Epstein, *Chaos* **18**, 026107 (2008).
- [8] H. J. Krug, L. Pohlmann, and L. Kuhnert, *J. Phys. Chem.* **94**, 4862 (1990).
- [9] V. S. Zykov, G. Bordiougov, H. Brandtstädter, I. Gerdes, and H. Engel, *Phys. Rev. Lett.* **92**, 018304 (2004).
- [10] V. Zykov and H. Engel, *Physica D* **199**, 243 (2004).
- [11] J. Schlesner, V. S. Zykov, H. Brandtstädter, I. Gerdes, and H. Engel, *New J. Phys.* **10**, 015003 (2008).
- [12] T. Sakurai, E. Mihaliuk, F. Chirila, and K. Showalter, *Science* **296**, 2009 (2002).
- [13] E. Mihaliuk, T. Sakurai, F. Chirila, and K. Showalter, *Phys. Rev. E* **65**, 065602 (2002).
- [14] J. Wolff, A. G. Papathanasiou, H. H. Rotermund, G. Ertl, X. Li, and I. G. Kevrekidis, *Phys. Rev. Lett.* **90**, 018302 (2003).
- [15] J. Wolff, A. G. Papathanasiou, I. G. Kevrekidis, H. H. Rotermund, and G. Ertl, *Science* **294**, 134 (2001).
- [16] J. Wolff, A. G. Papathanasiou, H. H. Rotermund, G. Ertl, M. A. Katsoulakis, X. Li, and I. G. Kevrekidis, *Phys. Rev. Lett.* **90**, 148301 (2003).
- [17] H. E. Nistazakis, P. G. Kevrekidis, B. A. Malomed, D. J. Frantzeskakis, and A. R. Bishop, *Phys. Rev. E* **66**, 015601 (2002).
- [18] B. Malomed, D. Frantzeskakis, H. Nistazakis, A. Yannacopoulos, and P. Kevrekidis, *Phys. Lett. A* **295**, 267 (2002).
- [19] P. Kevrekidis, I. Kevrekidis, B. Malomed, H. Nistazakis, and D. Frantzeskakis, *Phys. Scr.* **69**, 451 (2004).
- [20] J. Löber and H. Engel, *Phys. Rev. Lett.* **112**, 148305 (2014).
- [21] R. Buchholz, H. Engel, E. Kammann, and F. Tröltzsch, *Comput. Optim. Appl.* **56**, 153 (2013).
- [22] F. Tröltzsch, *Optimal control of partial differential equations*, Vol. 112 (American Mathematical Society, Providence, 2010).
- [23] J. Nocedal and S. J. Wright, *Numerical optimization*, Vol. 2 (Springer New York, 1999).
- [24] J. Löber, *Phys. Rev. E* **89**, 062904 (2014).
- [25] J. Keener, *SIAM Journal on Applied Mathematics* **46**, 1039 (1986).
- [26] I. V. Biktasheva, Y. E. Elkin, and V. N. Biktashev, *Phys. Rev. E* **57**, 2656 (1998).
- [27] V. S. Zykov, A. S. Mikhailov, and S. C. Müller, *Phys. Rev. Lett.* **81**, 2811 (1998).
- [28] D. Horváth, V. Petrov, S. K. Scott, and K. Showalter, *J. Chem. Phys.* **98**, 6332 (1993).
- [29] A. Malevanets, A. Careta, and R. Kapral, *Phys. Rev. E* **52**, 4724 (1995).
- [30] M. Kardar, G. Parisi, and Y.-C. Zhang, *Phys. Rev. Lett.* **56**, 889 (1986).
- [31] L. Schimansky-Geier, A. S. Mikhailov, and W. Ebeling, *Ann. Phys. (Leipzig)* **495**, 277 (1983).
- [32] A. Engel, *Phys. Lett. A* **113**, 139 (1985).
- [33] A. Engel and W. Ebeling, *Phys. Lett. A* **122**, 20 (1987).
- [34] A. Kulka, M. Bode, and H.-G. Purwins, *Phys. Lett. A* **203**, 33 (1995).
- [35] M. Bode, *Physica D* **106**, 270 (1997).
- [36] S. Alonso, J. Löber, M. Bär, and H. Engel, *Eur. Phys. J. Spec. Top.* **187**, 31 (2010).
- [37] J. Löber, M. Bär, and H. Engel, *Phys. Rev. E* **86**, 066210 (2012).
- [38] See Supplemental Material for movies.
- [39] F. Schlögl, *Z. Phys.* **253**, 147 (1972).
- [40] Y. B. Zeldovich and D. A. Frank-Kamenetskii, *Dokl. Akad. Nauk SSSR* **19**, 693 (1938).
- [41] A. Mikhailov, *Foundations of synergetics I: Distributed active systems* (Springer-Verlag, New York, 1990).
- [42] R. FitzHugh, *Biophys. J.* **1**, 445 (1961).
- [43] J. Nagumo, S. Arimoto, and S. Yoshizawa, *Pro. IRE* **50**, 2061 (1962).
- [44] D. Lebiez and U. Brandt-Pollmann, *Phys. Rev. Lett.* **91**, 208301 (2003).
- [45] K. Theißen, *Optimale Steuerprozesse unter partiellen Differentialgleichungs-Restriktionen mit linear eingehender Steuerfunktion*, Ph.D. thesis, Westfälische Wilhelms-Universität Münster, Münster, Germany (2006).
- [46] A. J. Krener and A. Isidori, *Systems & Control Letters* **3**, 47 (1983).
- [47] H. K. Khalil and J. Grizzle, *Nonlinear systems*, Vol. 3 (Prentice hall Upper Saddle River, 2002).
- [48] R. Hermann and A. J. Krener, *Automatic Control, IEEE Transactions on* **22**, 728 (1977).
- [49] P. Turchin, *Complex population dynamics: a theoretical/empirical synthesis*, Vol. 35 (Princeton University Press, Princeton, 2003).

- [50] E. Ben-Jacob, I. Cohen, and H. Levine, *Advances in Physics* **49**, 395 (2000).
- [51] N. Bailey, *The Mathematical Theory of Infectious Diseases*, Mathematics in Medicine Series (Oxford University Press, 1987).
- [52] J. Sneyd and J. Keener, *Mathematical physiology* (Springer-Verlag, New York, 2008).
- [53] J. D. Murray, *Mathematical biology*, Vol. 3 (Springer-Verlag, Berlin, 1993).
- [54] S. Thakur and R. Kapral, *J. Chem. Phys.* **135**, 024509 (2011).
- [55] S. Thakur, J.-X. Chen, and R. Kapral, *Angew. Chem. Int. Ed.* **50**, 10165 (2011).
- [56] W. K. Burton, N. Cabrera, and F. C. Frank, *Philos. T. R. Soc. A* **243**, 299 (1951).
- [57] J. H. E. Cartwright, A. G. Checa, B. Escribano, and C. Ignacio Sainz-Díaz, *Philos. T. R. Soc. A* **370**, 2866 (2012).
- [58] S. C. Ferreira, M. L. Martins, and M. J. Vilela, *Phys. Rev. E* **65**, 021907 (2002).
- [59] R. Araujo and D. McElwain, *Bull. Math. Biol.* **66**, 1039 (2004).
- [60] S. Residori, *Phys. Rep.* **416**, 201 (2005).
- [61] F. Haudin, R. G. Elías, R. G. Rojas, U. Bortolozzo, M. G. Clerc, and S. Residori, *Phys. Rev. Lett.* **103**, 128003 (2009).
- [62] F. Haudin, R. G. Elías, R. G. Rojas, U. Bortolozzo, M. G. Clerc, and S. Residori, *Phys. Rev. E* **81**, 056203 (2010).
- [63] J. Löber, R. Coles, J. Siebert, H. Engel, and E. Schöll, “Control of chemical wave propagation,” (2014), arXiv:1403.3363.